An Ultrawideband Dual-Polarized Tightly Coupled Dipole Array (TCDA) With Wide Scanning Range

Liangliang Zhao, Hailiang Zhu, Can Ding, *Member, IEEE*, Ganyu Liu, Huiling Zhao, Jinchao Mou, and Y. Jay Guo, *Fellow, IEEE*

***Abstract*— This letter presents an ultra-wideband (UWB) dual-linearly-polarized tightly coupled dipole array (TCDA) designed for wide-angle scanning in both E and H planes. The proposed TCDA design achieves exceptional performance, boasting a bandwidth of 10.2:1 (1.3–13.3 GHz) and an active voltage standing wave ratio (VSWR) of less than 3 when scanning up to ±70° in both E and H planes. This superior performance is achieved through the incorporation of four new design elements: gradual shorting posts, resistance patches, a notched balun, and a composite double-layer superstrate. These design elements effectively suppress various resonances, improve impedance matching, and enhance beam scanning capabilities. The antenna element has dimensions of 0.43λc × 0.43λc × 0.57λc, where λc represents the free space wavelength at the center frequency of 7.3 GHz. A 12×12 element array was fabricated and tested, further validating the proposed TCDA's noteworthy features, including dual-polarization operation, ultra-wide bandwidth, and the widest scanning angle in both E- and H-planes.**

***Index Terms*—Common-mode (CM) suppression, dual-polarization, tightly coupled dipole array (TCDA), ultra-wideband, wide-angle scanning.**

I. Introduction

Wireless communication and detection systems in the future are expected to have multiple modules to cover different operating bands and scanning range. To accomplish this, a common approach is to use different groups of antennas as well as other RF/digital hardware to support them. However, this method will significantly increase the installation space and weight, which is undesirable in most applications. This work aims to pursue an alternative approach, which involves utilizing a single low-profile antenna array to cover the entire range of required operating bands while maintaining effective impedance matching and beam scanning capabilities.

Inspired by Wheeler's ideal current sheet array (CSA) concept [1], Munk proposed the tightly coupled dipole array (TCDA) with wideband and low-profile characteristics [2], which provides a potential solution to the aforementioned problem. The fundamental concept behind TCDA is to introduce interdigital capacitance between antenna elements, as originally proposed in earlier works on TCDA. This technique is used to counteract the effect of ground plane inductance and 4:1 bandwidth was achieved. Thereafter, various approaches have been proposed to improve the performance of TCDA in terms of the operating band, scanning range, and overall size. Design of dual-polarized TCDA with 10.5:1 bandwidth in the UHF–X band and ±60° scanning range in the E-, H-, and D-planes was presented in [3]. This work developed full circuit models to avoid time-consuming parameter optimizations. However, the impedance matching deteriorates when the beam scanning reaches up to ±60° and the use of a complicated balun adds to the complexity of design and fabrication. In [4], a wideband TCDA with a low height of 0.28 λ_c was achieved, utilizing a compact balun. Despite the low-profile, the relatively narrow operating bandwidth (5.5:1) and scanning range in the H plane (±55°) limit its use in practical application. To further widen the operating band, a TCDA with a polarization convertor (PC) was proposed in [5]. The effect of replacing the ground plane with a PC was studied, which is considered to be a special approach to avoid the ground plane reflection without inducing any ohmic losses. Although the impedance bandwidth and radiation efficiency have been significantly enhanced, the ±30° scanning range demonstrates the contradiction between impedance bandwidth and scanning angle range. Recent research on TCDA has been extended to millimeter-wave in [6], where 7.6:1 bandwidth (5.7 GHz–43.3 GHz) with active reflection coefficient less than −6 dB was achieved. However, the array is one dimensional (1×8) and single polarized subject to material property and fabrication process. From what has been discussed above, we can see that design of TCDA with dual-polarization, wide operation band, and wide scanning range has become a significant challenge in modern wireless systems.

In this letter, a dual-polarized TCDA with enhanced feeding network and composite dual-layer superstrate (CDS) is developed. Several design techniques have been employed to address the design challenges. Firstly, the end of dipoles has been tapered to provide smooth impedance transitions. Additionally, gradual shorting posts and resistance patches have been incorporated at the end of overlapping pads to eliminate the effect of common-mode (CM) resonance. Secondly, a tapered balun with a notch has been introduced to realize impedance transformation. Moreover, to further widen the scanning range without compromising the impedance matching, a CDS that contains two types of unit cells has been employed. The proposed TCDA achieves a 10.2:1 bandwidth (1.3–13.3 GHz) with active VSWR less than 3 and ±70° scanning range in both E and H planes. The final 12×12 array includes a 10×10 effective array, with the outermost elements being utilized as dummy elements to reduce edge effects. In addition, the entire structure is manufactured using the PCB process, resulting in a low-cost, low-profile, and lightweight design.

The remainder of the paper is organized as follows: Section II is dedicated to discussing the operating principle and configuration of the TCDA. In Section III, the fabrication, assembly, simulation, and measurement results of a 12×12 prototype are presented, including

This work was supported by the Beijing Nova Program under Grant Z201100006820130. (*Liangliang Zhao and Hailiang Zhu, joint first authors, contributed equally to this work.*) *(Corresponding author: Hailiang Zhu.)*

Liangliang Zhao, Hailiang Zhu, Ganyu Liu, and Huiling Zhao are with the School of Electronics and Information, Northwestern Polytechnical University, Xi'an 710129, China (e-mail: zll18@mail.nwpu.edu.cn; zhuhl@nwpu.edu.cn; liugy@mail.nwpu.edu.cn; zhhl@nwpu.edu.cn).

Can Ding and Y. Jay Guo are with the Globe Big Data Technologies Centre (GBDTC), University of Technology Sydney (UTS), Sydney 2007, Australia (email: can.ding@uts.edu.au, jay.guo@uts.edu.au).

Jinchao Mou is with the China Satellite Network Innovation Co., Ltd, Beijing 100029, China (e-mail: jasongor2021@163.com).

active VSWR, gain, radiation patterns, and beam scanning performances. Section IV draws conclusions from this study.

II. TCDA Operating Principle and Configuration

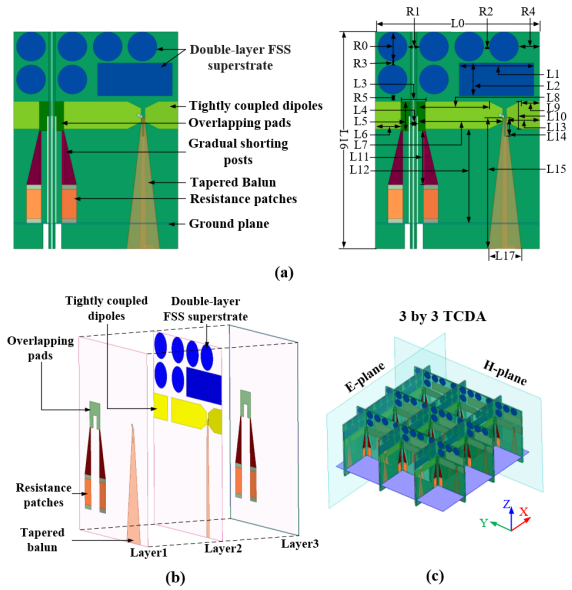

Fig. 1. Configuration of the proposed TCDA. (a) Side view of the element. (b) Exploded view of the element. (c) Example of a 3 × 3 array.

Fig. 1(a) shows the proposed dual-polarized TCDA element, which was constructed and analyzed as a periodically repeated unit. The element consists of a double-layer FSS superstrate, tightly coupled dipoles, overlapping pads, gradual shorting posts, tapered balun, resistance patches, and ground plane, arranged from top to bottom. The detailed values of the geometrical parameters are summarized in TABLE I. As seen in Fig. 1(b), the proposed TCDA is composed of three metal layers, hosted by two F4B substrates with a relative dielectric constant of 2.2 and a thickness of 0.254 mm. The overlapping pads, gradual shorting posts, resistance patches, and tapered balun are placed on the first layer. The double-layer FSS superstrate and tightly coupled dipoles are located on the second layer. Other sets of overlapping pads, gradual shorting posts, and resistance patches with same size as that of layer 1 appear on layer 3 again. Fig. 1 (c) illustrates the arrangement of a 3×3 array as an example.

A. Resonances suppression using GSPs, RPs, and a notch

It can be seen from Fig. 1 that the overlapping pads are printed on the first and third layers in parallel to overlap the dipole arms for capacitive coupling enhancement [7]. The length of the dipole is less than λ_h (λ_h is the free space wavelength at the upper frequency of the operation band) to avoid grating lobes. The ground plane under the dipole acts as a reflector which will introduce inductive coupling. As a result, the capacitive and inductive coupling effects counteract each other by turning the distance between the dipoles and the ground plane, leading to a good impedance matching over the ultra-wide band. However, as the bandwidth is further broadened, the presence of vertical unbalanced feeding lines leads to the occurrence of a common-mode (CM) resonance at a higher frequency band.

To address this issue, the proposed dual-polarized TCDA undergoes an evolutionary improvement, as illustrated in Fig. 2. In Design I, a widely used approach in previous TCDA designs involves the incorporation of a pair of shorting posts between the overlapping pads and the ground plane to mitigate the impedance mismatch issue.

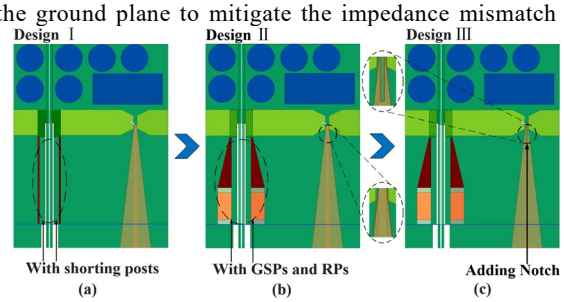

Fig. 2. Evolvement of the TCDA geometry to suppress unwanted resonances.

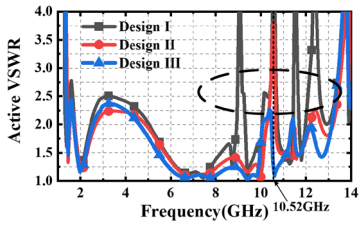

Fig. 3. Active VSWRs of the different designs.

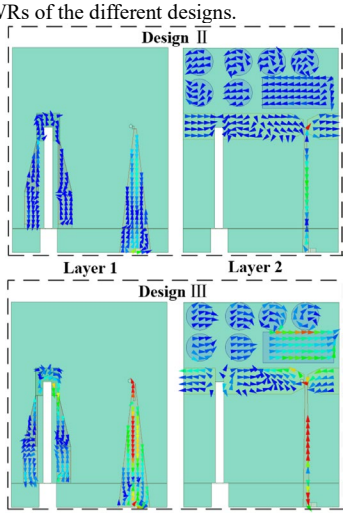

Fig. 4. Current distributions on Designs I and II at 10.52 GHz.

However, as shown in Fig. 3, this method alone is insufficient in effectively resolving the resonance problem.

In this work (Design II), the introduction of gradual shorting posts (GSPs) and resistance patches (RPs) offers a solution. As depicted in Fig. 3, the inclusion of GSPs and RPs successfully suppresses most of the CM resonances at the high frequency band.

Despite successfully suppressing three out of the four major resonances in Design I, the resonance at 10.52 GHz remains unchanged in Design II. To address this issue, Design III incorporates a rectangular notch on the balun, effectively mitigating the resonance problem. This improvement is confirmed by the VSWR results shown in Fig. 3 and the comparison of the current distribution in Fig. 4. To further illustrate how the notch in Design III suppresses the resonance at 10.52 GHz, Fig. 5 compares the real and imaginary parts of the input impedances for the three designs. It can be observed that the three designs exhibit similar resistance values, but the reactance has been reduced to zero in Design III due to the capacitance introduced by the notch at the resonance point.

Additionally, it should be noted that the results presented from Fig. 3 to Fig. 5 are for the E-plane only, but the same results hold true for the H-plane due to the symmetry of the proposed design.

TABLE I
Optimized Design Parameters Shown In Fig. 2.

Parameter	R0	R1	R2	R3	R4	R5	L0	L1	L2	L3	L4	L5
Value(mm)	3.2	1.34	0.67	0.4	2.3	0.8	18	8.18	3.6	2.68	1	3.2

Parameter	L6	L7	L8	L9	L10	L11	L12	L13	L14	L15	L16	L17
Value(mm)	2.8	9.3	7.8	2.1	3	5.9	10.3	3.6	2	14.3	23.7	3.6

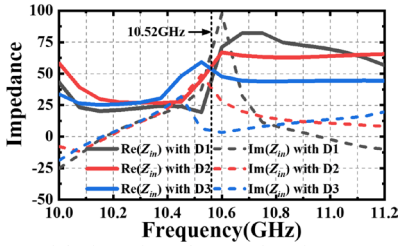

Fig. 5. Comparison of the input impedances of Designs I, II, and III.

B. Wide-angle scanning with composite double-layer superstrate (CDS)

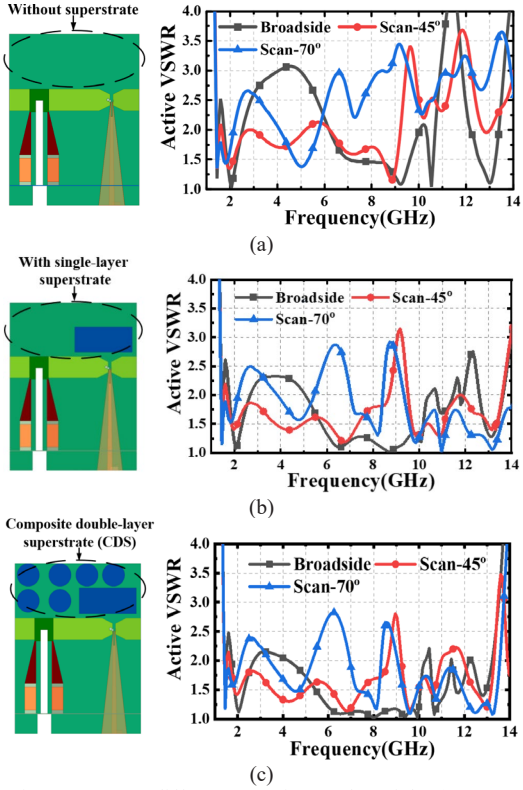

Fig. 6. Active VSWRs at different scanning angles of the (a) TCDA without superstrate, (b) TCDA with single-layer superstrate, and (c) TCDA with CDS.

Dielectric superstrates are commonly used to improve the scanning performance of TCDA. However, traditional dielectric slabs are usually thick and bulky, add complexity to the assembly manufacture, and can also result in trapped waves in the substrate at wide scanning angles. In this work, as shown in Fig. 1(a), a superstrate is developed to improve the scanning performance of the TCDA element while also maintaining impedance matching at wide scanning angles. This superstrate is designed on the same PCB layer as the TCDA element, making it easy to integrate. Fig. 6 demonstrates the impact of different superstrate designs on the active VSWR of the TCDA at various scanning angles (0°, 45°, 70°). In Fig. 6(a), without a superstrate, the TCDA exhibits impedance mismatching at all scanning angles. By introducing a rectangular patch unit on top of the dipole, as shown in Fig. 6(b), the mismatching is resolved when the beam direction aligns with the boresight. However, when the TCDA is scanned to larger angles, resonances occur at lower frequencies. Generally, as the scanning angle increases, more resonances occur at lower frequencies. In Fig. 6(c), the addition of circular patches, along with the rectangular patch, forms a CDS. This configuration mitigates the resonances when scanning to wide angles, ensuring that the active VSWR remains below 3 within an ultra-wide bandwidth. In summary, the proposed design achieves a bandwidth spanning more than a decade with a super wide scanning angle of up to ±70°.

III. Simulated and Experimental Results

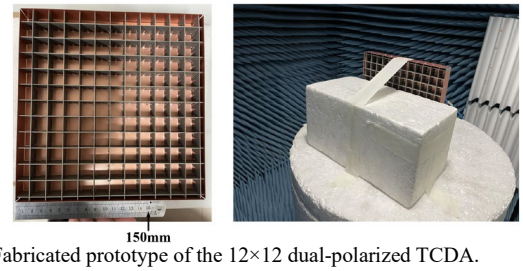

Fig. 7. Fabricated prototype of the 12×12 dual-polarized TCDA.

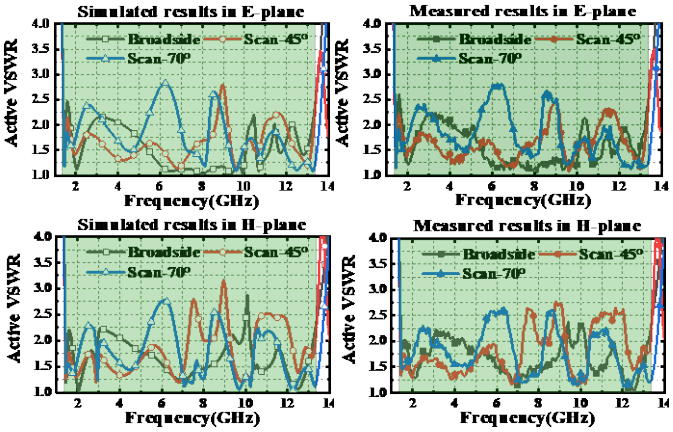

Fig. 8. Simulated VSWRs of the infinite TCDA (left) and the measured active VSWRs of the center element (right).

Fig. 7 depicts the fabricated prototype of the proposed antenna and its measurement environment. The dual-polarized TCDA prototype consists of 12×12 antenna elements, but to minimize the impact of array edge effects, dummy elements and metal walls are added at the edges. In each measurement, there were two active elements connected to vector network analyzer (VNA) and the rest 98 nonactive elements were terminated with 50 Ω loads. The active reflection coefficient for the i^{th} element, while scanning to the (θ_o, φ_o) direction, can be estimated using the equation given in [9]:

$$\Gamma_a(\theta_o,\varphi_o)=\sum_{n=1}^{N} S_{ni}\left|a_n\right|e^{-jk_o(xd_x\sin\theta_o\cos\varphi_o+ydy\sin\theta_o\cos\varphi_o)} \quad (1)$$

where S_{ni} is the measured complex coupling coefficients between the i^{th} element and the other elements of the array, $|a_n|$ represents the magnitude of the excitation of the radiating element, N is the total number of elements, k_o represents the free-space wavenumber, x and y are the element numbers, and dx and dy are the element spacings along the x-and y-directions, respectively. Furthermore, to characterize the radiation patterns of TCDA, the unit excitation active element pattern method [10] is utilized.

Fig. 8 shows the simulated and measured active VSWRs of the center element when the array is scanned to broadside, 45°, and 70° in the E-plane and H-plane, respectively. The measurement results agree well with the simulations. Please note that the final operating bandwidth, spanning from 1.3 to 13.3 GHz (10.2:1), is highlighted in green in the figure. Fig. 8 demonstrates that the measured active VSWR remains below 3 throughout the entire bandwidth, validating

the effectiveness of the proposed techniques for wide-angle scanning at various scanning angles. Meanwhile, there are some ripples in the measured results, which can be attributed to diffraction along the ground plane and the edges of the array. The measurement results demonstrate that the array performances for the two polarizations are consistent, which is due to the symmetry in antenna configuration.

The normalized patterns of the antenna scanning from broadside to 70° in E- and H-planes are shown in Fig. 9 and 10, respectively, at various frequencies. The comparison between the simulated and

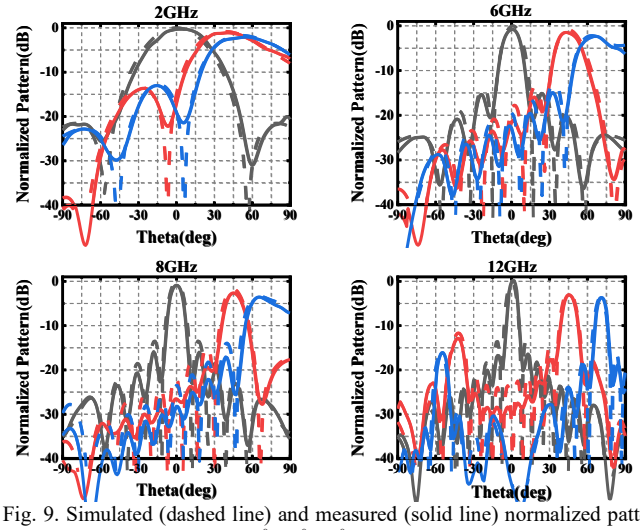

Fig. 9. Simulated (dashed line) and measured (solid line) normalized patterns in E-plane when scanning to 0^0, 45^0, 70^0 at 2, 6, 8, and 12 GHz.

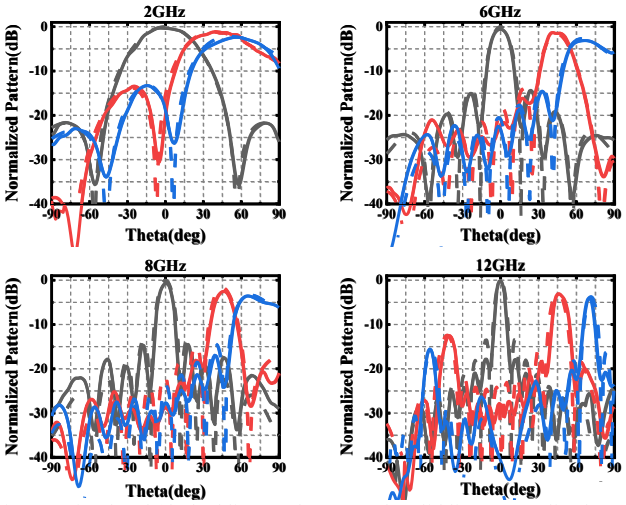

Fig. 10. Simulated (dashed line) and measured (solid line) normalized patterns in H-plane when scanning to 0^0, 45^0, 70^0 at 2, 6, 8, 12 GHz.

measured results show good agreement, as demonstrated in the figures.

Fig. 11 presents the simulated and measured realized gains of the TCDA when scanning in E-plane at 0°, 45°, and 70°. The corresponding results when scanning in H-plane are very similar and are not included here for brevity. The measured co-polarized gains exhibit good agreement with the simulated results. Additionally, the measured cross-polarization levels remain at least 20 dB below the co-polarization realized gains across the entire operating bandwidth, which is consistent with the simulation results.

To highlight the advantages of the proposed TCDA, a comparison is made with state-of-the-art designs in TABLE II. The proposed T C D A

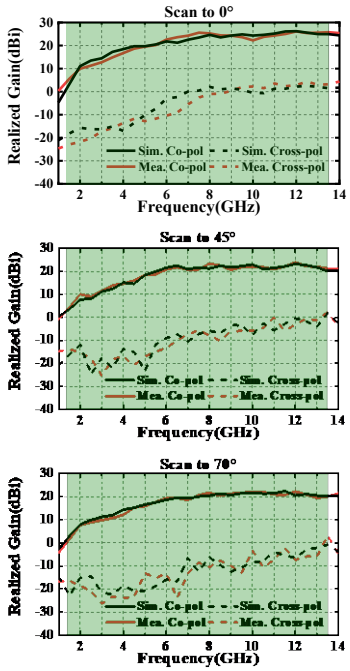

Fig. 11. Simulated and measured co-pol and cross-pol realized gains when scanning to 0^0, 45^0, and 70^0.

stands out for its dual-polarization operation, ultra-wide bandwidth, and widest scanning angle in both E- and H-planes. Among the dual-polarized TCDA designs, it also demonstrates the lowest VSWR across one of the widest achieved operating bandwidths.

IV. Conclusion

This work presents the design of a tightly coupled dipole array (TCDA) specifically optimized for wide-angle scanning in both E- and H-planes, supporting two linear polarizations, and operating within an ultra-wide bandwidth. To ensure good impedance matching across the entire bandwidth ranging from 1.3 to 13.3 GHz, several design techniques were employed. Gradual shorting posts (GSPs) and resistive patches (RPs) were utilized to effectively suppress common-mode resonances within the TCDA. Additionally, a notch was introduced in the balun to provide additional capacitance and mitigate a remaining resonance. To enable wide-angle scanning, a composite double-layer superstrate (CDS) was developed to suppress additional resonances occurring at lower frequencies when scanning at larger angles. A 12×12 array prototype was fabricated and measured to validate the performance of the design. Compared to state-of-the-art TCDA designs, this dual-polarized TCDA achieved the widest scanning angle of ±70° in both E- and H-planes, along with one of the widest operating bandwidths, maintaining a VSWR of less than 3. Notably, this design boasts a low-profile (0.57 λc), and ease of fabrication.

TABLE II
COMPARISON BETWEEN THE PROPOSED TCDA AND OTHER STATE-OF-THE-ART TCDA DESIGNS

Ref.	Bandwidth(broadside)	Profile	Scanning	Polarization
[15]	2.7:1 (2.2-6 GHz, VSWR < 2)	0.57 λ_c	E-45° (VSWR < 2)	Single-pol
[16]	4:1 (0.5-2 GHz, VSWR < 2)	0.41 λ_c	E-60°/H-60° (VSWR < 3)	Single-pol
[21]	7.33:1 (0.3–2.15 GHz, VSWR < 3)	0.82 λ_c	E-70°/H-50° (VSWR < 3)	Single-pol
[22]	3:1 (6-18 GHz, VSWR < 3)	0.29 λ_c	E-60°/H-60° (VSWR < 3)	Single-pol

[7]	8.5:1 (2.1-18 GHz, VSWR < 3)	0.51 λ_c	E-60°/H-30° (VSWR < 4)	Dual-pol
[25]	4.5:1 (4-18GHz, VSWR < 3.5)	0.33 λ_c	E-60°/H-45° (VSWR < 3.5)	Dual-pol
[26]	8:1 (2.6-21.2, VSWR<3.2)	1.01λ_c	E-45°/H-45° (VSWR < 3.8)	Dual-pol
This work.	**10.2:1 (1.3-13.3 GHz, VSWR < 3)**	**0.57 λ_c**	**E-70°/H-70° (VSWR < 3)**	**Dual-pol**

λ_c is the wavelength at the center frequency of the operating band.

REFERENCES

[1] B. Munk et al., "A low-profile broadband phased array antenna," *in IEEE Antennas Propag. Soc. Int. Symp. Dig. Held Conjunction USNC/CNC/URSI North Amer. Radio Sci. Meeting*, vol. 2, Jun. 2003, pp. 448–451.

[2] B. A. Munk, *Finite Antenna Arrays and FSS*. New York, NY, USA: Wiley, 2003.

[3] W. Zhou, Y. Chen and S. Yang, "Dual-Polarized Tightly Coupled Dipole Array for UHF–X-Band Satellite Applications," *IEEE Antennas Wireless Propag. Lett*., vol. 18, no. 3, pp. 467-471, March. 2019.

[4] A. O. Bah, P. -Y. Qin, R. W. Ziolkowski, Y. J. Guo and T. S. Bird, "A Wideband Low-Profile Tightly Coupled Antenna Array With a Very High Figure of Merit," *IEEE Trans Antennas Propag*., vol. 67, no. 4, pp. 2332-2343, April. 2019.

[5] S. Kim and S. Nam, "Characteristics of TCDA With Polarization Converting Ground Plane," *IEEE Trans Antennas Propag*., vol. 69, no. 4, pp. 2359-2364, April. 2021.

[6] J. Wang, X. Zhao, Y. Ye and S. Liu, "A Millimeter-Wave Ultrawideband Tightly Coupled Dipole Array Antenna for Vehicle Communication," *IEEE Antennas Wireless Propag. Lett*., vol. 21, no. 10, pp. 2135-2139, Oct. 2022.

[7] J. Zhong, A. Johnson, E. A. Alwan and J. L. Volakis, "Dual-Linear Polarized Phased Array With 9:1 Bandwidth and 60° Scanning Off Broadside," *IEEE Trans Antennas Propag*., vol. 67, no. 3, pp. 1996-2001, March. 2019.

[8] S. S. Holland and M. N. Vouvakis, "The Banyan Tree Antenna Array," *IEEE Trans Antennas Propag*., vol. 59, no. 11, pp. 4060-4070, Nov. 2011.

[9] M. N. Vouvakis and D. H. Schaubert, "Vivaldi antenna arrays," *in Frontiers in Antennas: Next Generation Design Engineering*, F. B. Gross, Ed. New York, NY, USA: McGraw-Hill, 2011.

[10] D. Pozar, "The active element pattern," *IEEE Trans Antennas Propag*., vol. 42, no. 8, pp. 1176–1178, Aug. 1994.

[11] J. P. Doane, K. Sertel and J. L. Volakis, "A Wideband, Wide Scanning Tightly Coupled Dipole Array With Integrated Balun (TCDA-IB)," *IEEE Trans Antennas Propag*., vol. 61, no. 9, pp. 4538-4548, Sept. 2013.

[12] W. F. Moulder, K. Sertel and J. L. Volakis, "Ultrawideband Superstrate-Enhanced Substrate-Loaded Array With Integrated Feed," *IEEE Trans Antennas Propag*., vol. 61, no. 11, pp. 5802-5807, Nov. 2013.

[13] M. H. Novak and J. L. Volakis, "Ultrawideband Antennas for Multiband Satellite Communications at UHF–Ku Frequencies," *IEEE Trans Antennas Propag*., vol. 63, no. 4, pp. 1334-1341, April. 2015.

[14] D. K. Papantonis and J. L. Volakis, "Dual-Polarized Tightly Coupled Array With Substrate Loading," *IEEE Antennas Wireless Propag. Lett*., vol. 15, pp. 325-328, 2016.

[15] Y. Wang, L. Zhu, H. Wang, Y. Luo and G. Yang, "A Compact, Scanning Tightly Coupled Dipole Array With Parasitic Strips for Next-Generation Wireless Applications," *IEEE Antennas Wireless Propag. Lett*., vol. 17, no. 4, pp. 534-537, April. 2018.

[16] H. Zhang, S. Yang, Y. Chen, J. Guo and Z. Nie, "Wideband Dual-Polarized Linear Array of Tightly Coupled Elements," *IEEE Trans Antennas Propag*., vol. 66, no. 1, pp. 476-480, Jan. 2018.

[17] H. Zhang, S. Yang, S. Xiao, Y. Chen and S. Qu, "Low-Profile, Lightweight, Ultra-Wideband Tightly Coupled Dipole Arrays Loaded With Split Rings," *IEEE Trans Antennas Propag*., vol. 67, no. 6, pp. 4257-4262, June 2019.

[18] A. D. Johnson, J. Zhong, S. B. Venkatakrishnan, E. A. Alwan and J. L. Volakis, "Phased Array With Low-Angle Scanning and 46:1 Bandwidth," *IEEE Trans Antennas Propag*., vol. 68, no. 12, pp. 7833-7841, Dec. 2020.

[19] S. Kim and S. Nam, "Compact Ultrawideband Antenna on Folded Ground Plane," *IEEE Trans Antennas Propag*., vol. 68, no. 10, pp. 7179-7183, Oct. 2020.

[20] B. Wang, S. Yang, Z. Zhang, Y. Chen, S. Qu and J. Hu, "A Ferrite-Loaded Ultralow Profile Ultrawideband Tightly Coupled Dipole Array," *IEEE Trans Antennas Propag*., vol. 70, no. 3, pp. 1965-1975, March. 2022.

[21] H. Zhang, S. Yang, S. -W. Xiao, Y. Chen, S. -W. Qu and J. Hu, "Ultrawideband Phased Antenna Arrays Based on Tightly Coupled Open Folded Dipoles," *IEEE Antennas Wireless Propag. Lett*., vol. 18, no. 2, pp. 378-382, Feb. 2019.

[22] Z. Zhang, M. Huang, Y. Chen, S. -W. Qu, J. Hu and S. Yang, "In-Band Scattering Control of Ultra-Wideband Tightly Coupled Dipole Arrays Based on Polarization-Selective Metamaterial Absorber," *IEEE Trans Antennas Propag*., vol. 68, no. 12, pp. 7927-7936, Dec. 2020.

[23] E. Yetisir, N. Ghalichechian and J. L. Volakis, "Ultrawideband Array With 70° Scanning Using FSS Superstrate," *IEEE Trans Antennas Propag*., vol. 64, no. 10, pp. 4256-4265, Oct. 2016.

[24] F. Yang, B. Wang, Y. Chen, S. Qu and S. Yang, "An Effective Optimization Methods for the Suppression of Edge Effects in Ultrawideband Tightly Coupled Antenna Arrays," *IEEE Trans Antennas Propag*., vol. 70, no. 12, pp. 11639-11652, Dec. 2022.

[25] J. X. Sun, Y. J. Cheng and Y. Fan, "Planar Ultra-Wideband and Wide-Scanning Dual-Polarized Phased Array With Integrated Coupled-Marchand Balun for High Polarization Isolation and Low Cross-Polarization," *IEEE Trans Antennas Propag*., vol. 69, no. 11, pp. 7134-7144, Nov. 2021.

[26] R. W. Kindt and J. T. Logan, "Dual-Polarized Metal-Flare Sliced Notch Antenna Array," *IEEE Trans Antennas Propag*., vol. 68, no. 4, pp. 2666-2674, April. 2020.